IMA Journal of Applied Mathematics (2019) **00**, 1–27
doi:10.1093/imamat/hxz022

Large-time dynamics in complex networks of reaction–diffusion systems applied to a panic model

GUILLAUME CANTIN*, M.A. AZIZ-ALAOUI AND NATHALIE VERDIÈRE
Laboratoire de Mathématiques Appliquées du Havre, Normandie University, Fédération de Recherche Institut des Systémes Complexes en Normandie 3335, ISCN, 76600 Le Havre, France
*Corresponding author: guillaumecantin@mail.com

[Received on 1 December 2018; revised on 26 April 2019; accepted on 15 August 2019]

This paper is devoted to the analysis of the asymptotic behaviour of a complex network of reaction–diffusion systems for a geographical model, which was proposed recently, in order to better understand behavioural reactions of individuals facing a catastrophic event. After stating sufficient conditions for the problem to admit a positively invariant region, we establish energy estimates and prove the existence of a family of exponential attractors. We explore the influence of the size of the network on the nature of those attractors, in correspondence with the geographical background. Numerical simulations illustrate our theoretical results and show the various possible dynamics of the problem.

Keywords: dynamical system; complex network; asymptotic behaviour; reaction–diffusion; attractor; panic model.

1. Introduction

The Panic–Control–Reflex (PCR) system is a mathematical model for understanding behavioural reactions of individuals facing catastrophic events (Cantin *et al.*, 2016; Provitolo *et al.*, 2015) that can have a natural or industrial cause. The original association of geographers, computer scientists and mathematicians has produced this new model, which is given by the following system of ordinary differential equations, where the unknown functions r, c, p and q denote, respectively, the subpopulations of individuals in 'reflex', 'control', 'panic' and 'daily' behaviours:

$$\dot{u} = \Phi(u, t), \tag{1.1}$$

where $u = (r, c, p, q)^T$ and Φ is defined by

$$\Phi(u, t) = \begin{pmatrix} -Br + \gamma(t)q(1-r) + frc + grp \\ B_1 r - C_2 c + C_1 p - frc + hcp - \varphi(t)c(r+c+p+q) \\ B_2 r - C_1 p + C_2 c - grp - hcp \\ -\gamma(t)q(1-r) \end{pmatrix}, \tag{1.2}$$

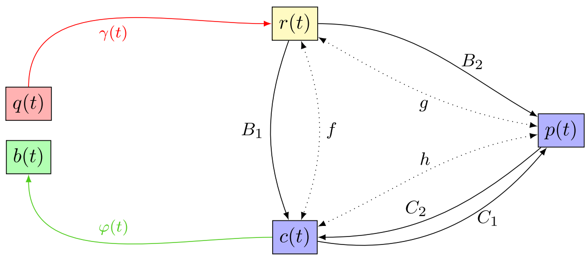

FIG. 1. Flux diagram for the PCR system, showing behavioural evolutions and imitation phenomena among the subgroups q (daily behaviour before the catastrophe), r (reflex), c (control), p (panic) and b (daily behaviour after the catastrophe). Source: Provitolo *et al.* (2015).

with positive bounded functions $\gamma(t)$, $\varphi(t)$, which model, respectively, the beginning and the end of the catastrophic event, positive coefficients $B_i > 0$, $C_i > 0$, $i \in \{1, 2\}$, $B = B_1 + B_2$, which model the evolution processes among the behavioural subgroups, and real coefficients f, g, h, which correspond to the imitation phenomena that act in parallel. The PCR system is derived from the following five equations system:

$$\begin{cases} \dot{r} = -Br + \gamma(t)q(1-r) + frc + grp \\ \dot{c} = B_1 r - C_2 c + C_1 p - frc + hcp - \varphi(t)c(b_m - b) \\ \dot{p} = B_2 r - C_1 p + C_2 c - grp - hcp \\ \dot{q} = -\gamma(t)q(1-r) \\ \dot{b} = +\varphi(t)c(b_m - b), \end{cases} \tag{1.3}$$

where b denotes the subpopulation of individuals in daily behaviour ‘after’ the catastrophic event, which is assumed to occur for a limited time. The distinction between b and the subgroup q of individuals before the catastrophe corresponds to the assumption that individuals who have been subject to a behavioural loop caused by the catastrophic event, and who succeed to return to the daily behaviour, will not be subject to a second behavioural loop. Finally, b_m corresponds to the maximal number of individuals who can evolve from the control behaviour c to the daily behaviour b. The whole process occurring among the behavioural subgroups is depicted in Fig. 1. We suppose that the maximal capacity b_m coincides with the total population, i.e.

$$b_m = r + c + p + q + b. \tag{1.4}$$

We emphasize that b_m can be a function of time t, especially in the case of coupled networks of PCR systems. Equation (1.4) implies the reduction $b_m - b = r + c + p + q$, which leaves the fifth equation in (1.3) governed by the rest of the system, thus we eliminate it, and finally obtain system (1.1).

The PCR system has been studied in collaboration with geographers and computers scientists, in order to analyse various situations of catastrophic events. Its mathematical analysis is presented in Cantin *et al.* (2016), where the authors show that the system admits two classes of solutions, depending on whether the value of the evolution parameter C_1 from panic behaviour to control behaviour is positive or null. In the first case, i.e. $C_1 > 0$, it is proved that the solution converges to the trivial equilibrium, which corresponds to the expected situation when all individuals return to a daily behaviour. In the second case, when $C_1 = 0$, the system exhibits a persistence of panic, which is the situation that must be avoided, at the risk to worsen the impact of the catastrophic event. In that latter case, it was shown that the quadratic imitation terms can inhibit or exacerbate the persistence of panic, according to the direction of the imitation process from panic to control or from control to panic, respectively. The example of an earthquake in Japan is studied in Verdière *et al.* (2015). Since in Japan, the risk culture is well established, the population is trained to react quickly, thus the causality process from reflex or panic to control is important with respect to the other processes, even for a zone that is closed to the epicentre of the earthquake. The consideration of the geographical relief of the zone impacted by the catastrophe naturally leads to the study of coupled networks. Specific questions arise in the study of complex systems defined by such coupled networks, among them ‘synchronization’, or the relationship between the topology of the network and the dynamics of the system. In a recent conference paper (see Cantin *et al.*, 2017), another example concerning the particular risk of tsunami on the Mediterranean coast has been studied. It is shown in this latter article that the evacuation of high-risk zones corresponding to the beach places, towards the refuge zones situated in the city centre, plays a very decisive role. For instance, a plugged corridor can provoke a persistence of panic. At the opposite, an additional evacuation path from the beach towards the city centre can help individuals return to the daily behaviour. In Cantin (2017), those patterns are generalized in the case of any network.

In this paper, our aim is to improve the model, by taking into account the local displacements of individuals. Following the ‘random walk’ approach, we add a spatial diffusion term, as it has frequently been done in numerous mathematical models, with a physical, chemical, biological or ecological background (Murray, 2002; Okubo, 1980). Our approach results in a coupled network of reaction–diffusion systems, with a Neumann boundary condition that models the impossibility for individuals to leave or enter the area impacted by the catastrophe. It is well known that a richness of dynamics, such as travelling waves or Turing patterns, can occur in reaction–diffusion systems (Li *et al.*, 2013; Ruan, 1998; Sherratt, 2008), whereas it cannot be observed in systems involving only one of the two parts of the reaction–diffusion process. Nevertheless, original questions arise in the study of the dynamics of the network. Thus, we address at each step of our reasoning, a particular attention on the influence of the nature of the network.

This paper is organized as follows. In the next section, we present the two reaction–diffusion problems that we focus on, which are the PCR system with diffusion, and the corresponding network problem endowed with linear coupling terms. We indicate the functional spaces context, show that those problems are well-posed and demonstrate the non-negativity of the solutions starting from initial conditions with non-negative components. In Section 3, we explore sufficient conditions for the solutions to evolve in positively invariant regions, which guarantees their existence in the large, and we analyse their asymptotic behaviour, by stating energy estimates and proving the existence of a family of exponential attractors. Each theorem is discussed in relationship with the geographical background of our model. In the final section, we show various numerical simulations in order to illustrate our theoretical results. Those simulations have been prepared with the collaboration of geographers (see Cantin *et al.*, 2017; Provitolo *et al.*, 2015) and are related to the realistic scenario of a tsunami on the Mediterranean coast.

2. Problem statement and preliminaries

2.1 *PCR system with diffusion*

Let us consider an open bounded subset $\Omega \subset \mathbb{R}^2$ with regular boundary $\partial\Omega$ and the initial-boundary value problem

$$\begin{cases} r_t = d_1 \Delta r - Br + \gamma q(1-r) + frc + grp & \text{in } \Omega \times (0,\infty) \\ c_t = d_2 \Delta c + B_1 r - C_2 c + C_1 p - frc + hcp - \varphi c(r+c+p+q) & \text{in } \Omega \times (0,\infty) \\ p_t = d_3 \Delta p + B_2 r - C_1 p + C_2 c - grp - hcp & \text{in } \Omega \times (0,\infty) \\ q_t = d_4 \Delta q - \gamma q(1-r) & \text{in } \Omega \times (0,\infty) \\ \dfrac{\partial r}{\partial \nu} = \dfrac{\partial c}{\partial \nu} = \dfrac{\partial p}{\partial \nu} = \dfrac{\partial q}{\partial \nu} = 0 & \text{on } \partial\Omega \times (0,\infty) \\ r(x,0) = r_0(x),\ c(x,0) = c_0(x), & \\ p(x,0) = p_0(x),\ q(x,0) = q_0(x) & \text{in } \Omega, \end{cases} \tag{2.1}$$

where the diffusion rates d_i are positive (> 0), $1 \leqslant i \leqslant 4$, B_1, B_2, $B = B_1 + B_2$, C_1, C_2 are positive coefficients. For simplicity, we reduce our study to the case where the functions γ, φ are positive constants such that

$$0 < \gamma \leqslant 1, \quad 0 < \varphi \leqslant 1, \tag{2.2}$$

which implies that system (2.1) is autonomous. This reduction is reasonable, since it is proved in Cantin (2017) that replacing γ and φ by positive constants does not change the asymptotic dynamics of the system. However, we indicate that this assumption can be weakened (see Yagi, 2009, Section 6 in Chapter IV for existence results, and Efendiev *et al.*, 2005 or Caraballo *et al.*, 2006 for the concept of attractor for non-autonomous systems). The coefficients f, g, and h involved in the interactions among the three behavioural subgroups r, c and p, are assumed to satisfy

$$-1 \leqslant f \leqslant 1, \quad -1 \leqslant g \leqslant 1, \quad -1 \leqslant h \leqslant 1. \tag{2.3}$$

Finally, $\frac{\partial}{\partial \nu}$ denotes the derivative with respect to the outward normal tangent to $\partial\Omega$.

Remark 1 The domain Ω models the zone that is impacted by the catastrophe. Its shape and size have an influence on the spectral properties of the diffusion operator Δ and can vary according to the geographical landscape. In the example of a tsunami on the Mediterranean coast, the steps corridors between the beach places and the city centre are of particular interest. Their dimensions represent a key factor in the evacuation of the high-risk zones. Typically, the values of the diffusion rates d_i, $1 \leqslant i \leqslant 4$, will be different for each behavioural subgroup. More precisely, we will focus on the situation when the diffusion rate d_2 corresponding to the control behaviour is larger than the diffusion rate d_3 corresponding to the panic behaviour, whereas the diffusion rates d_1 and d_4 corresponding to the reflex and daily behaviours, will have a small value. Nevertheless, it is worth noting that this modelling choice represents a rough approximation, since the panic behaviour subgroup could be divided into different sub-classes, for instance ‘flight’ panic or ‘prostration’ panic.

2.2 *Abstract formulation of the PCR system*

Following Yagi (2009), we formulate system (2.1) as a Cauchy problem for a semi-linear equation. Thus, we consider the Banach space of complex valued functions

$$X = \left(L^2(\Omega)\right)^4, \tag{2.4}$$

equipped with the product norm of $L^2(\Omega)$, defined by

$$\|u\|_X = \left(\sum_{i=1}^{4} \|u_i\|^2_{L^2(\Omega)}\right)^{\frac{1}{2}},$$

for all $u = (u_i)_{1\leqslant i\leqslant 4} \in X$. Next we introduce the diagonal operator

$$A = \mathrm{diag}(A_i, 1 \leqslant i \leqslant 4),$$

where $A_i, 1 \leqslant i \leqslant 4$, are the realizations of $-d_1\Delta + B$, $-d_2\Delta + C_2$, $-d_3\Delta + C_1$ and $-d_4\Delta + \gamma$, respectively, in $L^2(\Omega)$, under Neumann boundary conditions on $\partial\Omega$.

The operators A_i, $1 \leqslant i \leqslant 4$, are positive definite self-adjoint operators of $L^2(\Omega)$ (see Yagi, 2009, Theorem 2.6), with domain

$$H^2_N(\Omega) = \left\{u \in H^2(\Omega);\ \frac{\partial u}{\partial \nu} = 0 \text{ on } \partial\Omega\right\}. \tag{2.5}$$

Hence, A is a positive definite self-adjoint operator of the product space X.

We fix $\eta \in \left]\frac{3}{4}, 1\right[$, and consider the fractional power operator A^η, whose domain is given by the interpolation space (see Yagi, 2009, Theorem 16.7)

$$\mathcal{D}(A^\eta) = \left(\left[L^2(\Omega),\ H^2_N(\Omega)\right]_\eta\right)^4 = \left(H^{2\eta}_N(\Omega)\right)^4, \tag{2.6}$$

with the norm equivalence

$$\frac{1}{c_0}\|u\|_{H^{2\eta}(\Omega)} \leqslant \left\|A_i^\eta u\right\|_{L^2(\Omega)} \leqslant c_0\|u\|_{H^{2\eta}(\Omega)}, \tag{2.7}$$

for all $u \in \mathcal{D}\left(A_i^\eta\right)$, $1 \leqslant i \leqslant 4$, for a given constant $c_0 > 0$. Since $2\eta > 1$ and Ω is bounded, the embedding theorems for Sobolev spaces (Adams & Fournier, 2003; Yagi, 2009) guarantee that

$$H^{2\eta}(\Omega) \subset \mathscr{C}\left(\overline{\Omega}\right), \tag{2.8}$$

with continuous embedding. Additionally, due to the boundedness of Ω, it is clear that

$$\mathscr{C}\left(\overline{\Omega}\right) \subset L^\infty(\Omega) \subset L^2(\Omega), \tag{2.9}$$

with continuous embeddings.

Next we consider the nonlinear operator $F = \left(F_i\right)_{1 \leqslant i \leqslant 4}$ defined on $\mathcal{D}\left(A^{\eta}\right)$ by

$$F(v) = \begin{pmatrix} \gamma q(1-r) + frc + grp \\ B_1 r + C_1 p - f(rc + hcp - \varphi c(r + c + p + q) \\ B_2 r + C_2 c - grp - hcp \\ \gamma qr \end{pmatrix}, \tag{2.10}$$

for all $t > 0$ and $v = (r, c, p, q)^T \in \mathcal{D}\left(A^{\eta}\right)$. Finally, we introduce the space of initial values, defined by

$$X_0 = \left\{ U_0 = (r_0, c_0, p_0, q_0)^T \in X; r_0 \geqslant 0, c_0 \geqslant 0, p_0 \geqslant 0, q_0 \geqslant 0 \right\}. \tag{2.11}$$

Thus, we can formulate (2.1) as a semi-linear parabolic equation in X:

$$(I) \begin{cases} \dfrac{\mathrm{d}U}{\mathrm{d}t} + AU = F(U), \quad t > 0, \\ U(0) = U_0. \end{cases} \tag{2.12}$$

REMARK 2 The choice of exponent $\eta \in \left]\frac{3}{4}, 1\right[$ corresponds to a double constraint. On the one hand, $\eta > \frac{3}{4}$ guarantees embedding (2.8), which in turn implies

$$H^{2\eta}(\Omega) \subset L^{\infty}(\Omega).$$

On the other hand, $\eta < 1$ enables the use of a contraction mapping theorem for showing the existence and uniqueness of a local in time solution (see Theorems 1 and 2 below).

2.3 *Coupled network problem*

In this section, our aim is to model the geographical area impacted by the catastrophic event, by taking into account the heterogeneous distribution of individuals on different places. Thus, we define a coupled network problem by considering a graph $\mathscr{G} = \left(\mathscr{N}, \mathscr{E}\right)$ made with a finite set $\mathscr{N}$ of n nodes ($n \in \mathbb{N}^*$) and a finite set $\mathscr{E}$ of edges. This network model has already been studied in Cantin (2017), in the case of ordinary differential equations. Here we intend to improve the network model by coupling multiple instances of reaction–diffusion system (2.1). Let us describe how nodes and edges can model the geographical landscape.

First, each node of the network is associated with one region of the geographical area, which can be modelled by a bounded domain $\Omega_i \subset \mathbb{R}^2$, $1 \leqslant i \leqslant n$. For instance, those domains can correspond to beaches, step corridors or city centre places. For the sake of simplicity, we reduce our analysis by assuming that the domains Ω_i, $1 \leqslant i \leqslant n$ are identical to a generic domain Ω. We emphasize that this assumption is common in the study of coupled networks of reaction–diffusion systems, among them neural networks (see Yang *et al.*, 2013; Wang *et al.*, 2018; Ambrosio *et al.*, 2019). The dynamics of each node is determined by a reaction–diffusion process involving the function $\Phi^{(i)}$ defined by

$$\Phi^{(i)}(U_i) = \begin{pmatrix} -B^{(i)} r_i + \gamma q_i(1 - r_i) + f r_i c_i + g r_i p_i \\ B_1^{(i)} r_i - C_2^{(i)} c_i + C_1^{(i)} p_i - f r_i c_i + h c_i p_i - \varphi c_i(r_i + c_i + p_i + q_i) \\ B_2^{(i)} r_i + C_2^{(i)} c_i - C_1^{(i)} p_i - g r_i p_i - h c_i p_i \\ -\gamma q_i(1 - r_i) \end{pmatrix},$$

where $U_i = (r_i, c_i, p_i, q_i)^T$ determines the state of node i ($1 \leqslant i \leqslant n$) and an above index (i) that indicates that the parameters B_1, B_2, C_1 and C_2 are not necessarily equal for different nodes. This implies that two distinct nodes in the network can exhibit two different dynamics, according to the corresponding parameters values. For instance, some nodes associated with exposed areas could present a persistence of panic, while other nodes associated with refuge zones would present a return to the daily behaviour. In particular, we are interested in finding sufficient conditions on the topology of the network so that the persistence of panic is limited at an arbitrary level.

Next each edge of the network is associated with one connection between a pair of nodes and models physical displacements of individuals from one node to another. For instance, one edge can model a street connecting a beach to a city centre place. We fix $\varepsilon > 0$, and we introduce the matrix of connectivity $L = \big(L_{i,j}\big)_{1 \leqslant i,j \leqslant n}$ by setting

$$L_{j,i} = \varepsilon \text{ if } (i,j) \in \mathscr{E} \text{ with } i \neq j, \quad L_{i,i} = -\sum_{\substack{j=1 \\ j \neq i}}^{n} L_{j,i}, \tag{2.13}$$

thus L is a matrix of order n whose sum of coefficients of each column is null (Hale, 1997). We assume that the set of edges $\mathscr{E}$ does not possess any loop. We also consider the coupling matrix $\mathcal{H}$ of order 4 defined by

$$\mathcal{H} = \operatorname{diag}\big(1, 1, 1, 0\big), \tag{2.14}$$

which indicates that the components r, c and p are coupled, but not q, since the individuals in daily behaviour are almost concerned with an instantaneous evolution towards the reflex behaviour, rather than moving to other places.

The equations of the network problem read

$$\frac{\partial U_i}{\partial t} = D\Delta U_i + \Phi^{(i)}(U_i) + \sum_{j=1}^{n} L_{i,j}\mathcal{H}U_j, \quad 1 \leqslant i \leqslant n, \quad \text{in } \Omega \times (0, \infty), \tag{2.15}$$

where $U_i = (r_i, c_i, p_i, q_i)^T$, $D = \operatorname{diag}(d_1, d_2, d_3, d_4)$, with the Neumann boundary condition

$$\frac{\partial r_i}{\partial \nu} = \frac{\partial c_i}{\partial \nu} = \frac{\partial p_i}{\partial \nu} = \frac{\partial q_i}{\partial \nu} = 0, \quad 1 \leqslant i \leqslant n, \quad \text{on } \partial\Omega \times (0, \infty), \tag{2.16}$$

and initial conditions

$$\begin{aligned} & r_i(x,0) = r_{i,0}(x), \quad c_i(x,0) = c_{i,0}(x), \\ & p_i(x,0) = p_{i,0}(x), \quad q_i(x,0) = q_{i,0}(x), \quad 1 \leqslant i \leqslant n, \quad \text{in } \Omega. \end{aligned} \tag{2.17}$$

2.4 *Abstract formulation of the network problem*

We can write the network problem (2.15) as a Cauchy problem in X^n:

$$(II) \begin{cases} \dfrac{\mathrm{d}\mathscr{U}}{\mathrm{d}t} + \mathscr{A}\mathscr{U} = \mathscr{F}\left(\mathscr{U}\right), \quad t > 0, \\ \mathscr{U}(0) = \mathscr{U}_0, \end{cases} \tag{2.18}$$

where $\mathscr{U} = (U_1, \ldots, U_n)^T$, $\mathscr{A}$ is the diagonal operator defined by

$$\mathscr{A} = \operatorname{diag}(A^{(i)},\ 1 \leqslant i \leqslant n), \tag{2.19}$$

with domain $\mathcal{D}(\mathscr{A}) = \left(H^2_N(\Omega)\right)^n$, where

$$A^{(i)} = \operatorname{diag}(-d_1\Delta + B^{(i)}, -d_2\Delta + C_2^{(i)}, -d_3\Delta + C_1^{(i)}, -d_4\Delta + \gamma), \quad 1 \leqslant i \leqslant n.$$

Furthermore, $\mathscr{F}$ is the nonlinear operator defined in $\mathcal{D}\left(\mathscr{A}^\eta\right)$ by

$$\mathscr{F}(\mathscr{U}) = \left(F^{(i)}(U_i)\right)_{1\leqslant i\leqslant n} + \mathcal{L}(\mathscr{U}), \tag{2.20}$$

where η is fixed as previously such that $\frac{3}{4} < \eta < 1$, $\mathscr{U}_0 \in X_0^n$, $\mathcal{L}$ is given by

$$\mathcal{L}(\mathscr{U}) = \left(\sum_{j=1}^{n} L_{i,j}\mathcal{H}U_j\right)_{1\leqslant i\leqslant n}, \tag{2.21}$$

and $F^{(i)}$ coincides with the operator F defined by (2.10), except that the parameters B_1, B_2, C_1 and C_2 are supposed to depend on i.

In the rest of this paper, the symbols k_i, $i \in \mathbb{N}$, denote positive constants. In order to lighten our notations, we will write L^2, H^2, $H^{2\eta}$, etc. instead of $L^2(\Omega)$, $H^2(\Omega)$, $H^{2\eta}(\Omega)$, respectively. We shall need the following lemma for integrating differential inequalities (Yagi, 2009).

LEMMA 1 Assume that α, β and u are smooth real-valued functions defined on $[0,\ T]$, such that

$$\dot{u}(t) + \alpha(t)u(t) \leqslant \beta(t), \quad t \in [0,\ T].$$

Then we have

$$u(t) \leqslant u(0)\mathrm{e}^{-\int_0^t \alpha(s)\mathrm{d}s} + \int_0^t \beta(s)\mathrm{e}^{-\int_s^t \alpha(\theta)\mathrm{d}\theta}\mathrm{d}s, \quad t \in [0,\ T].$$

2.5 *Existence and uniqueness of local solutions*

In this section, we state and prove our first results that guarantee the existence and uniqueness of local solutions for the two previous problems (2.12) and (2.18). To that aim, we look for Lipschitz-type estimations of the nonlinear operators F and $\mathscr{F}$ by fractional powers of A and $\mathscr{A}$, respectively. We begin with an estimation of the first component of F.

LEMMA 2 There exists a positive constant κ_1 such that

$$\left\|F_1(v)-F_1(\tilde{v})\right\|_{L^2} \leqslant \kappa_1\Big[\left\|A^\eta(v-\tilde{v})\right\|_X+\left(\left\|A^\eta v\right\|_X+\left\|A^\eta \tilde{v}\right\|_X\right)\|v-\tilde{v}\|_X\Big],$$

for all $v, \tilde{v} \in \mathcal{D}(A^\eta)$.

Proof. Let us consider $v=(r, c, p, q)^T$, $\tilde{v}=(\tilde{r}, \tilde{c}, \tilde{p}, \tilde{q})^T \in \mathcal{D}\left(A^\eta\right)$. We write

$$\left\|F_1(v)-F_1(\tilde{v})\right\|_{L^2} \leqslant\|\gamma q-\gamma \tilde{q}\|_{L^2}+\|\gamma q r-\gamma \tilde{q} \tilde{r}\|_{L^2}+\|f r c-f \tilde{r} \tilde{c}\|_{L^2}+\|g r p-g \tilde{r} \tilde{p}\|_{L^2}.$$

First, we have

$$\|\gamma q-\gamma \tilde{q}\|_{L^2} \leqslant \gamma\|q-\tilde{q}\|_{L^2} \leqslant\|q-\tilde{q}\|_{L^2} \leqslant k_1\left\|A^\eta(v-\tilde{v})\right\|_X,$$

and analogously,

$$\begin{aligned}
\|\gamma q r-\gamma \tilde{q} \tilde{r}\|_{L^2} & \leqslant\|q r-q \tilde{r}\|_{L^2}+\|q \tilde{r}-\tilde{r} \tilde{q}\|_{L^2} \\
& \leqslant k_2\Big[\|q\|_{H^{2\eta}}\|r-\tilde{r}\|_{L^2}+\|\tilde{r}\|_{H^{2\eta}}\|q-\tilde{q}\|_{L^2}\Big] \\
& \leqslant k_3\left(\left\|A^\eta v\right\|_X+\left\|A^\eta \tilde{v}\right\|_X\right)\|v-\tilde{v}\|_X .
\end{aligned}$$

In the mean time, we have

$$\begin{aligned}
\|f r c-f \tilde{r} \tilde{c}\|_{L^2} & \leqslant|f|\,\|r c-\tilde{r} \tilde{c}\|_{L^2} \\
& \leqslant k_4\Big[\|r c-r \tilde{c}\|_{L^2}+\|r \tilde{c}-\tilde{r} \tilde{c}\|_{L^2}\Big] \\
& \leqslant k_5\left(\left\|A^\eta v\right\|_X+\left\|A^\eta \tilde{v}\right\|_X\right)\|v-\tilde{v}\|_X,
\end{aligned}$$

and similarly,

$$\|g r p-g \tilde{r} \tilde{p}\|_{L^2} \leqslant k_6\left(\left\|A^\eta v\right\|_X+\left\|A^\eta \tilde{v}\right\|_X\right)\|v-\tilde{v}\|_X .$$

It follows that

$$\left\|F_1(v)-F_1(\tilde{v})\right\|_{L^2} \leqslant k_7\Big[\left\|A^\eta(v-\tilde{v})\right\|_X+\left(\left\|A^\eta v\right\|_X+\left\|A^\eta \tilde{v}\right\|_X\right)\|v-\tilde{v}\|_X\Big].$$

□

Following the same method, we obtain similar estimations for F_i, involving positive constants κ_i, $2 \leqslant i \leqslant 4$. Finally, we introduce $\kappa_0 = \max(\kappa_i, 1 \leqslant i \leqslant 4)$, which leads to

$$\|F(v) - F(\tilde{v})\|_X \leqslant \kappa_0 \Big[\left\|A^\eta (v - \tilde{v})\right\|_X + \left(\left\|A^\eta v\right\|_X + \left\|A^\eta \tilde{v}\right\|_X \right) \|v - \tilde{v}\|_X \Big], \tag{2.22}$$

for all $v, \tilde{v} \in \mathcal{D}(A^\eta)$.

THEOREM 1 For any $U_0 \in X_0$, there exists $T_{U_0} > 0$ such that the semi-linear Cauchy problem (2.12) admits a unique solution U in the function space

$$\mathscr{C}\big((0, T_{U_0}], \mathcal{D}(A)\big) \cap \mathscr{C}\big([0, T_{U_0}], X\big) \cap \mathscr{C}^1\big((0, T_{U_0}], X\big). \tag{2.23}$$

Furthermore, U satisfies the estimate

$$t\,\|AU(t)\|_X \leqslant C_{U_0}, \quad \forall\, t \in]0, T_{U_0}], \tag{2.24}$$

where C_{U_0} is a positive constant depending on U_0.

Proof. The operator A is sectorial with angle $\omega_A < \frac{\pi}{2}$ (see Haase, 2006; Yagi, 2009). Following Yagi (2009, Chapter 4, Theorem 4.4), we can deduce from the Lipschitz estimation (2.22) the existence and uniqueness of a local solution U in space (2.23), with estimation (2.24). □

Similarly, we show that the network problem (2.18) admits local solutions.

THEOREM 2 For any $\mathscr{U}_0 \in X_0^n$, there exists $T_{\mathscr{U}_0} > 0$ such that the semi-linear Cauchy problem (2.18) admits a unique solution $\mathscr{U}$ in the function space

$$\mathscr{C}\big((0, T_{\mathscr{U}_0}], \mathcal{D}(\mathscr{A})\big) \cap \mathscr{C}\big([0, T_{\mathscr{U}_0}], X^n\big) \cap \mathscr{C}^1\big((0, T_{\mathscr{U}_0}], X^n\big). \tag{2.25}$$

Furthermore, $\mathscr{U}$ satisfies the estimate

$$t\,\|\mathscr{A}\mathscr{U}(t)\|_X \leqslant C_{\mathscr{U}_0}, \quad \forall\, t \in]0, T_{\mathscr{U}_0}], \tag{2.26}$$

where $C_{\mathscr{U}_0}$ is a positive constant depending on $\mathscr{U}_0$.

Proof. We examine the coupling terms stored in $\mathscr{F}$. For $v_i, \tilde{v}_i \in \mathcal{D}(A^\eta)$, we have

$$\left\| \sum_{j=1}^n L_{i,j}\mathcal{H}v_i - \sum_{j=1}^n L_{i,j}\mathcal{H}\tilde{v}_i \right\|_X \leqslant \|L\|_{\mathscr{M}_n(\mathbb{R})} \sum_{j=1}^n \left\|v_i - \tilde{v}_i\right\|_X, \tag{2.27}$$

for each i such that $1 \leqslant i \leqslant n$, where $\|\cdot\|_{\mathscr{M}_n(\mathbb{R})}$ denotes any norm on the space of matrices of order n with real coefficients. Combined, with the estimation (2.22), we obtain

$$\|\mathscr{F}(v) - \mathscr{F}(\tilde{v})\|_{X^n} \leqslant k_8\Big[\, \big\|\mathscr{A}^\eta(v-\tilde{v})\big\|_{X^n} + \big(\big\|\mathscr{A}^\eta v\big\|_{X^n} + \big\|\mathscr{A}^\eta \tilde{v}\big\|_{X^n}\big)\, \|v-\tilde{v}\|_{X^n}\Big],$$

for all $v, \tilde{v} \in \mathcal{D}(\mathscr{A}^\eta)$. The operator $\mathscr{A}$ being sectorial with angle $\omega_{\mathscr{A}} < \frac{\pi}{2}$, we obtain as previously the expected statements. □

In the rest of the paper, the letters U and $\mathscr{U}$ will be reserved for the solutions of problems (2.12) and (2.18), respectively.

3. Sufficient conditions for the existence of an invariant region

3.1 *Non-negativity*

In this section, we prove the non-negativity of the solutions U and $\mathscr{U}$ of both problems (2.12) and (2.18) starting from $U_0 \in X_0$ and $\mathscr{U}_0 \in X_0^n$, respectively, which is an obvious property to be satisfied for a population dynamics model.

We recall that a nonlinear operator $\Phi = (\Phi_i)_{1\leqslant i\leqslant m}$ defined on $\mathbb{R}^m$ (with $m \in \mathbb{N}^*$) is said to be 'quasi-positive' if it satisfies the property

$$\Phi_i(u_1, \ldots, u_{i-1}, 0, u_{i+1}, \ldots, u_m) \geqslant 0, \tag{3.1}$$

for all $u = (u_1, \ldots, u_m) \in (\mathbb{R}^+)^m$ and for all $i \in \{1, \ldots, m\}$. The quasi-positivity of the nonlinear operator Φ defined by (1.2) is a necessary and sufficient condition for proving the non-negativity property of the solutions of system (2.1) (Pierre, 2010; Rothe, 1984).

Proposition 1 Let $U_0 \in X_0$, and U be the solution of problem (2.12) starting from U_0, defined on $[0, T_{U_0}]$. Then its components r, c, p and q are non-negative on $[0, T_{U_0}]$.

Proof. Let $(r, c, p, q)^T \in (\mathbb{R}^+)^4$. We have

$$\begin{aligned}
\Phi_1(0, c, p, q) &= \gamma q \geqslant 0,\\
\Phi_2(r, 0, p, q) &= B_1 r + C_1 p \geqslant 0,\\
\Phi_3(r, c, 0, q) &= B_2 r + C_1 c \geqslant 0,\\
\Phi_4(r, c, p, 0) &= 0,
\end{aligned}$$

which means that Φ is quasi-positive and implies the non-negativity of r, c, p and q on $[0, T_{U_0}]$. □

In the same manner, we easily prove the non-negativity property for the solution $\mathscr{U}$ of the network problem (2.18).

Proposition 2 Let $\mathscr{U}_0 \in X_0^n$, and $\mathscr{U}$ be the solution of problem (2.18) starting from $\mathscr{U}_0$, defined on $[0, T_{\mathscr{U}_0}]$. Then its components r_i, c_i, p_i and q_i, $1 \leqslant i \leqslant n$ are non-negative on $[0, T_{\mathscr{U}_0}]$.

Proof. Let $(r_i, c_i, p_i, q_i)_{1\leqslant i\leqslant n} \in (\mathbb{R}^+)^{4n}$. The form of the connectivity matrix L defined by (2.13) and of the matrix $\mathcal{H}$ defined by (2.14) leads to

$$\Phi_1^{(i)}\big((r_1, c_1, p_1, q_1), \dots, (0, c_i, p_i, q_i), \dots, (r_n, c_n, p_n, q_n)\big) = \gamma q_i + \sum_{\substack{j=1\\ j\neq i}}^{n} L_{i,j} r_j \geqslant 0,$$

$$\Phi_2^{(i)}\big((r_1, c_1, p_1, q_1), \dots, (r_i, 0, p_i, q_i), \dots, (r_n, c_n, p_n, q_n)\big) = B_1^{(i)} r_i + C_1^{(i)} p_i + \sum_{\substack{j=1\\ j\neq i}}^{n} L_{i,j} c_j \geqslant 0,$$

$$\Phi_3^{(i)}\big((r_1, c_1, p_1, q_1), \dots, (r_i, c_i, 0, q_i), \dots, (r_n, c_n, p_n, q_n)\big) = B_2^{(i)} r_i + C_1^{(i)} c_i + \sum_{\substack{j=1\\ j\neq i}}^{n} L_{i,j} p_j \geqslant 0,$$

$$\Phi_4^{(i)}\big((r_1, c_1, p_1, q_1), \dots, (r_i, c_i, p_i, 0), \dots, (r_n, c_n, p_n, q_n)\big) = 0,$$

for all $i \in \{1, \dots, n\}$, which guarantees the non-negativity of each component of $\mathscr{U}$ on $[0, T_{\mathscr{U}_0}]$. □

3.2 *Invariant regions and existence in the large*

Our aim in this section is to give sufficient conditions for the two problems (2.12) and (2.18) to admit an invariant region. We introduce for $\alpha > 0$ and $\beta > 0$ the compact subset $R_{\alpha,\beta}$ of $\mathbb{R}^4$ defined by

$$R_{\alpha,\beta} = [0, 1] \times [0, \alpha] \times [0, \beta] \times [0, 1]. \tag{3.2}$$

Let $\mu = \max\big(|f|, |g|, |h|\big)$, and assume $\mu \leqslant \frac{\varphi}{2}$.

THEOREM 3 Suppose that the following assumptions hold:

$$\mu(\alpha + \beta) < B, \tag{3.3}$$

$$B_1 \leqslant (\varphi - \mu)\alpha, \quad C_1 \leqslant (\varphi - \mu)\alpha, \tag{3.4}$$

$$\mu < \frac{C_1}{1+\alpha}, \quad \beta > \frac{B_2 + C_2\alpha}{C_1 - \mu(1+\alpha)}. \tag{3.5}$$

Then the compact set $R_{\alpha,\beta}$ is positively invariant under the flow induced by the problem (2.12).

REMARK 3 The assumptions of the latter theorem are in conformity with the geographical background of our model and do not represent a major constraint. Indeed, the second assumption always holds provided α is chosen sufficiently large. Furthermore, the first and third assumptions are satisfied if μ is sufficiently small, which means that the imitation processes that take place among the three behavioural subgroups are of lesser intensity than the evolution phenomena, and if β is sufficiently large. The size of the compact set $R_{\alpha,\beta}$ varies with α and β. If the action of φ is weak, then the value of α is required to be large with respect to B_1 and C_1. This means that the control component c can admit large values in the case of a weak behavioural purge. Meanwhile, if the value of the evolution parameter C_1 from panic to control is small, then the value of β is required to be large with respect to B_2 and C_2, thus a difficult evolution from panic to control can provoke a high level of panic.

Proof of Theorem 3. For $U_0 \in X_0$, let $U = (r, c, p, q)^T$ be the solution of problem (2.12), defined on $[0, T_{U_0}]$. We successively examine each component of the solution $U = (r, c, p, q)$, so the proof is divided into four steps. It suffices to verify that the vector field corresponding to the reaction part of the system strictly points into the interior of $R_{\alpha,\beta}$ (see Smoller, 1994). If it is tangent in some places of its boundary, we can use a cut-off method (see Yagi, 2009).

First step. The first equation in the system (2.12) reads

$$\frac{\partial r}{\partial t} = d_1 \Delta r + \Phi_1(U),$$

with $\Phi_1(U) = -Br + \gamma q(1-r) + frc + grp$ [see equation (1.2)]. If there exists t^* such that $r(t^*) = 1$, then we have

$$\Phi_1\big(U(t^*)\big) = -B + fc(t^*) + gp(t^*) \leqslant -B + \mu(\alpha+\beta) < 0,$$

according to equation (3.3), which guarantees that $r(t) \leqslant 1$ for all $t \in [0, T_{U_0}]$. We have already proved the non-negativity of U, so we obtain

$$0 \leqslant r(t) \leqslant 1, \quad t \in [0, T_{U_0}].$$

Second step. Next we consider the fourth equation in the system (2.12):

$$\frac{\partial q}{\partial t} = d_4 \Delta q + \Phi_4(U),$$

with $\Phi_4(U) = -\gamma q(1-r)$. We introduce $\xi = 1 - q$ and the function ρ defined by

$$\rho(t) = \int_\Omega \chi(\xi)\mathrm{d}x,$$

where χ is a cut-off function defined on $\mathbb{R}$ by

$$\chi(x) = \begin{cases} 0 & \text{if} x > 0, \\ \frac{1}{2}x^2 & \text{if} x \leqslant 0. \end{cases} \tag{3.6}$$

It is continuously differentiable on $\mathbb{R}$, with $\chi'(x) = 0$ if $x > 0$, $\chi'(x) = x$ if $x \leqslant 0$, and it satisfies the properties

$$\chi(x) \geqslant 0, \quad \chi'(x) \leqslant 0, \quad 0 \leqslant \chi'(x)\,x \leqslant 2\chi(x), \quad \forall x \in \mathbb{R}. \tag{3.7}$$

We have $\rho(0) = 0$ because $q(0) \leqslant 1$, and obviously $\rho(t) \geqslant 0$ for all $t \in [0, T_{U_0}]$. We compute the derivative of $\rho(t)$:

$$\rho'(t) = \int_\Omega \chi'(\xi)\big[-d_4\Delta q + \gamma q(1-r)\big]\mathrm{d}x = d_4 \int_\Omega \chi'(\xi)\Delta\xi\,\mathrm{d}x + \gamma \int_\Omega \chi'(\xi)q(1-r)\mathrm{d}x.$$

Since we have

$$\int_{\Omega} \chi'(\xi)\Delta\xi \mathrm{d}x = -\int_{\Omega} \left|\nabla\chi'(\xi)\right|^2 \mathrm{d}x \leqslant 0,$$

and additionally $r \leqslant 1$, we conclude that $\rho \equiv 0$, i.e.

$$0 \leqslant q(t) \leqslant 1, \quad t \in [0, T_{U_0}].$$

Third step. Similarly, we set $\xi = \alpha - c$ and consider $\rho(t) = \int_{\Omega} \chi(\xi)\mathrm{d}x$. We have successively

$$\begin{aligned}\frac{\partial \xi}{\partial t} &= -\frac{\partial c}{\partial t}\\ &= -d_2\Delta c - B_1 r + C_2 c - C_1 p + frc - hcp + \varphi c(r + c + p + q)\\ &= d_2\Delta\xi + C_2 c + \varphi(c^2 + cq) - (B_1 - \varphi c - fc)r - (C_1 - \varphi c + hc)p.\end{aligned}$$

It follows that

$$\begin{aligned}\rho'(t) = d_2 \int_{\Omega} \chi'(\xi)\Delta\xi \mathrm{d}x + \int_{\Omega} \chi'(\xi)\big[C_2 c + \varphi(c^2 + cq)\big]\mathrm{d}x\\ - \int_{\Omega} \chi'(\xi)\left[(B_1 - \varphi c - fc)r + (C_1 - \varphi c + hc)p\right]\mathrm{d}x.\end{aligned}$$

Assumption (3.4) leads to

$$\chi'(\xi)(B_1 - \varphi c - fc)r \geqslant 0, \quad \chi'(\xi)(C_1 - \varphi c + hc)p \geqslant 0,$$

so we obtain

$$-\int_{\Omega} \chi'(\xi)\left[(B_1 - \varphi c - fc)r + (C_1 - \varphi c + hc)p\right]\mathrm{d}x \leqslant 0,$$

thus $\rho \equiv 0$ and finally,

$$0 \leqslant c(t) \leqslant \alpha, \quad t \in [0, T_{U_0}].$$

Fourth step. Using assumption (3.5), we prove in the same manner that

$$0 \leqslant p(t) \leqslant \beta, \quad t \in [0, T_{U_0}].$$

□

Now, we continue with the research of invariant regions for the network problem (2.18). In order to prove that the product set

$$\mathscr{R} = \prod_{1\leqslant i\leqslant n} R_{\alpha_i,\beta_i} \tag{3.8}$$

is a positively invariant region for the flow induced by (2.18), we need to make additional assumptions on the network, which are similar to Kirchoff-type requirements frequently met in graph theory (see Chen *et al.*, 2014). For each node $i \in \{1, \ldots, n\}$ of the network, let us introduce the subset $J_i \subset \{1, \ldots, n\}$ composed with all other nodes j ($j \neq i$), which enter into i, and inversely, the total coupling strength exiting from the node i, defined by $E_i = -L_{i,i}$ [see equation (2.13)].

THEOREM 4 Suppose that assumptions (3.3)–(3.5) hold for $i \in \{1, \dots, n\}$ and that additionally we have

$$\mu(\alpha_i + \beta_i) + \sum_{j \in J_i} L_{i,j} < B^{(i)} + E_i, \tag{3.9}$$

$$\sum_{j \in J_i} L_{i,j} < E_i + C_2^{(i)} + \varphi\alpha_i, \tag{3.10}$$

$$B_2^{(i)} + C_2^{(i)}\alpha_i + \mu(1+\alpha_i)\beta_i + \beta_i \sum_{j \in J_i} L_{i,j} < E_i\beta_i + C_1^{(i)}\beta_i, \tag{3.11}$$

for each node $i \in \{1, \dots, n\}$. Then the compact set $\mathscr{R}$ defined by (2.17) is positively invariant under the flow induced by the network problem (2.18).

The proof can be made by repeating the same arguments, so we omit it.

REMARK 4 The Kirchoff-type requirements (3.9)–(3.11) of Theorem 4 are easily satisfied for a node that plays the role of a 'source'. In that case, we have $E_i > 0$ and in the mean time, $\sum_{J_i} L_{i,j} = 0$. At the opposite, those requirements could be violated for a node that would play the role of a dead end. For those nodes, it is crucial that the value of the parameter $C_1^{(i)}$ is sufficiently large in counterpart of $E_i = 0$. In our application, the zones that are situated in a dead end are often refuge zones, which favours the evolution process from panic to control, thus a sufficiently large value of parameter C_1. In other words, the assumptions (3.9)–(3.11) are compatible with our model.

The latter statements allow us to construct semi-groups of nonlinear operators for both problems (2.12) and (2.18). Under the assumptions of Theorem 3, we have shown that the compact region $R_{\alpha,\beta}$ is positively invariant. We set

$$Z = L^2(\Omega, R_{\alpha,\beta}), \quad \mathscr{Z} = L^2(\Omega, \mathscr{R}).$$

For $U_0 \in Z$, let $U(t, U_0)$ be the solution of the problem (2.12) defined for all $t \geqslant 0$. We introduce the family of operators $S(t)$ acting on Z by setting

$$S(t)U_0 = U(t, U_0), \tag{3.12}$$

for all $t \geqslant 0$ and $U_0 \in Z$. The family $\big(S(t)\big)_{t \geqslant 0}$ defines a nonlinear semi-group acting on Z. Similarly, for $\mathscr{U}_0 \in \mathscr{Z}$, let $\mathscr{U}(t, \mathscr{U}_0)$ be the solution of the problem (2.18) defined for all $t \geqslant 0$. We set

$$\mathscr{S}(t)\mathscr{U}_0 = \mathscr{U}(t, \mathscr{U}_0), \tag{3.13}$$

for all $t \geqslant 0$ and $\mathscr{U}_0 \in \mathscr{Z}$.

4. Energy estimates and existence of attractors

In this section, our aim is to study the asymptotic behaviour of the solutions U and $\mathscr{U}$ of the problems (2.12) and (2.18). We suppose that U and $\mathscr{U}$ evolve in $R_{\alpha,\beta}$ and $\mathscr{R}$, respectively.

PROPOSITION 3 Assume that the assumptions of Theorem 3 hold. Let

$$\begin{aligned}\delta_0 &= \min\left(\frac{\gamma}{2},\, 2B-3-2\mu(\alpha+\beta)\right),\\ \delta_1 &= 2C_2-B_1-C_1,\\ \delta_2 &= 2C_1-B_2-C_2.\end{aligned}\tag{4.1}$$

Assume that $\delta_i > 0$ for $0 \leqslant i \leqslant 2$, $\delta_0 \neq \delta_1$ and $\delta_0 \neq \delta_2$. Then there exist positive constants K_i, $1 \leqslant i \leqslant 4$, such that

$$\begin{aligned}\frac{\gamma}{2}\,\|r(t)\|_{L^2}^2 + \|q(t)\|_{L^2}^2 &\leqslant \left(\frac{\gamma}{2}\,\|r_0\|_{L^2}^2 + \|q_0\|_{L^2}^2\right)\mathrm{e}^{-\delta_0 t}\\ \|c(t)\|_{L^2}^2 &\leqslant \|c_0\|_{L^2}^2\mathrm{e}^{-\delta_1 t} + K_3\frac{\mathrm{e}^{-\delta_0 t}-\mathrm{e}^{-\delta_1 t}}{\delta_1-\delta_0} + \frac{K_1}{\delta_1}\\ \|p(t)\|_{L^2}^2 &\leqslant \|p_0\|_{L^2}^2\mathrm{e}^{-\delta_2 t} + K_4\frac{\mathrm{e}^{-\delta_0 t}-\mathrm{e}^{-\delta_2 t}}{\delta_2-\delta_0} + \frac{K_2}{\delta_2},\end{aligned}\tag{4.2}$$

for all $t > 0$.

Proof. We introduce

$$\begin{aligned}R(t) &= \frac{1}{2}\int_\Omega \big(r(t)\big)^2\mathrm{d}x, \quad C(t) = \frac{1}{2}\int_\Omega \big(c(t)\big)^2\mathrm{d}x,\\ P(t) &= \frac{1}{2}\int_\Omega \big(p(t)\big)^2\mathrm{d}x, \quad Q(t) = \frac{1}{2}\int_\Omega \big(q(t)\big)^2\mathrm{d}x,\end{aligned}$$

where we omit the space variable x in order to lighten our notations. We first compute the derivative of R:

$$\begin{aligned}R'(t) &= \int_\Omega r(t)\frac{\partial r}{\partial t}(t)\mathrm{d}x\\ &= \int_\Omega d_1 r(t)\Delta r(t)\mathrm{d}x - B\int_\Omega \big(r(t)\big)^2\mathrm{d}x + \gamma\int_\Omega q(t)r(t)\big[1-r(t)\big]\mathrm{d}x\\ &\quad + \int_\Omega \Big[f\big(r(t)\big)^2 c(t) + g\big(r(t)\big)^2 p(t)\Big]\,\mathrm{d}x\\ &\leqslant -2BR(t) + \gamma\int_\Omega q(t)r(t)\mathrm{d}x - \gamma\int_\Omega q(t)\big(r(t)\big)^2\mathrm{d}x + 2\mu(\alpha+\beta)R(t)\\ &\leqslant \big(-2B+1+2\mu(\alpha+\beta)\big)R(t) + Q(t),\end{aligned}$$

for all $t > 0$, using the non-negativity of $q(t)$ and the inequality $ab \leqslant \frac{a^2}{2}+\frac{b^2}{2}$, a, $b \in \mathbb{R}$. It follows that

$$\frac{\gamma}{2}R'(t) \leqslant \frac{\gamma}{2}\big(-2B+1+2\mu(\alpha+\beta)\big)R(t) + \frac{\gamma}{2}Q(t),$$

for $t > 0$. Similarly, we obtain

$$Q'(t) \leqslant -\gamma Q(t) + \gamma R(t), \quad t > 0,$$

which leads to, after summing the two latter inequalities,

$$\frac{\gamma}{2}R'(t) + Q'(t) \leqslant \big(-2B + 3 + 2\mu(\alpha+\beta)\big)\frac{\gamma}{2}R(t) - \frac{\gamma}{2}Q(t), t > 0.$$

We introduce $\delta_0 = \min\left(\frac{\gamma}{2}, 2B - 3 - 2\mu(\alpha+\beta)\right)$, thus

$$\frac{\gamma}{2}R'(t) + Q'(t) \leqslant -\delta_0\left(\frac{\gamma}{2}R(t) + Q(t)\right), t > 0,$$

which yields, by virtue of Lemma (1),

$$\frac{\gamma}{2}\,\|r(t)\|_{L^2}^2 + \|q(t)\|_{L^2}^2 \leqslant \left(\frac{\gamma}{2}\,\|r_0\|_{L^2}^2 + \|q_0\|_{L^2}^2\right)\mathrm{e}^{-\delta_0 t},$$

for all $t > 0$. Next we compute $C'(t)$ and $P'(t)$:

$$\begin{aligned}
C'(t) &= \int_\Omega c(t)\frac{\partial c}{\partial t}(t)\mathrm{d}x \\
&= \int_\Omega c(t)\big[d_2\Delta c(t) - C_2 c(t) + B_1 r(t) + C_1 p(t)\big]\mathrm{d}x \\
&\quad + \int_\Omega \big[-f\times r(t)\big(c(t)\big)^2 + h\times\big(c(t)\big)^2 p(t)\big]\mathrm{d}x - \varphi\int_\Omega c(t)^2\big[r(t)+c(t)+p(t)+q(t)\big]\mathrm{d}x \\
&\leqslant -2C_2C(t) + B_1R(t) + B_1C(t) + C_1P(t) + C_1C(t) + \mu\alpha^2(1+\beta)\,|\Omega| \\
&\leqslant -(2C_2 - B_1 - C_1)C(t) + B_1R(t) + C_1P(t) + \mu\alpha^2(1+\beta)\,|\Omega| \\
&\leqslant -\delta_1 C(t) + k_9\mathrm{e}^{-\delta_0 t} + K_1,
\end{aligned}$$

for $t > 0$, with $\delta_1 = 2C_2 - B_1 - C_1$ and

$$K_1 = \left[\frac{\beta^2 C_1}{2} + \mu\alpha^2(1+\beta)\right]|\Omega|, \tag{4.3}$$

and we obtain the desired estimate

$$\|c(t)\|_{L^2}^2 \leqslant \|c_0\|_{L^2}^2\mathrm{e}^{-\delta_1 t} + K_3\frac{\mathrm{e}^{-\delta_0 t} - \mathrm{e}^{-\delta_1 t}}{\delta_1 - \delta_0} + \frac{K_1}{\delta_1},$$

for all $t > 0$, by using Lemma (1). In the same manner, we have

$$P'(t) \leqslant -\delta_2 P(t) + k_10\mathrm{e}^{-\delta_0 t} + K_2,$$

for $t > 0$, with $\delta_2 = 2C_1 - B_2 - C_2$ and

$$K_2 = \left[\frac{\alpha^2 C_2}{2} + \mu\beta^2(1+\alpha)\right]|\Omega|, \tag{4.4}$$

which leads to

$$\|p(t)\|^2_{L^2} \leqslant \|p_0\|^2_{L^2}\mathrm{e}^{-\delta_2 t} + K_4\frac{\mathrm{e}^{-\delta_0 t} - \mathrm{e}^{-\delta_2 t}}{\delta_2 - \delta_0} + \frac{K_2}{\delta_2},$$

for all $t > 0$. The proof is complete. □

REMARK 5 The first estimation in (4.2) guarantees that the components r and q for the reflex and daily behaviours exponentially tend to 0 if $\delta_0 > 0$, at a speed that increases with B and γ, which concords with the observations of geographers. At the opposite, the estimates for the control and panic behaviours c and p, as given by the expressions (4.2), contain residual terms that let various asymptotic behaviours be possible. The constants K_1 and K_2 given by (4.3) and (4.4) are proportional to $|\Omega|$. Hence, when the size of Ω tends to 0, it is reasonable to expect that c and p converge to 0, accordingly to the behaviour of the solution of the ODE system in the general case $C_1 > 0$ mentioned in our introduction. In the estimate for the control component c, the residual term is the ratio $\frac{K_1}{\delta_1}$. But δ_1 increases with the value of the parameter C_2, which models the evolution process from control to panic. Thus, the residual term for the estimate of the control component c is as small as C_2 is large. In the estimate for the panic component p, the residual term is the ratio $\frac{K_2}{\delta_2}$. If C_1 tends to 0, δ_2 can be negative, and the estimate fails to prove that p converges to 0. In the mean time, β can increase [see Remark (3)], which implies a larger value for K_1, thus a possible positive limit for c. Roughly speaking, a small value for C_1 can provoke a persistence of panic and that persistence can postpone the decrease of c. Once again, the evolution parameter from panic to control C_1 is identified to play a crucial role in the asymptotic behaviour of our model.

Next we state energy estimates for the solution $\mathscr{U}$ of the network problem (2.18). Similar arguments are used for the proof. For that reason, we may omit it.

PROPOSITION 4 Assume that the assumptions of Theorem 4 hold. Then the solution $\mathscr{U}$ of the network problem (2.15) starting form $\mathscr{U}_0 \in \mathscr{X}$ satisfies

$$\|\mathscr{U}(t)\|^2_{X^n} \leqslant \|\mathscr{U}_0\|^2_{X^n}\mathrm{e}^{-2k_0 t} + \frac{Z_0}{2k_0}, \tag{4.5}$$

for $t > 0$, with $k_0 = \min(B^{(i)}, C_2^{(i)}, C_1^{(i)}, \gamma, 1 \leqslant i \leqslant n)$, and Z_0 is given by

$$Z_0 = 4n \max(1, \alpha_i, \beta_i, 1 \leqslant i \leqslant n)\ |\Omega| \left(\max_{1\leqslant i\leqslant n} \sup_{R_{\alpha_i,\beta_i}} \left|F^{(i)}\right| + \sup_{\mathscr{R}} |\mathcal{L}|\right). \tag{4.6}$$

REMARK 6 The energy estimate (4.5) and the expression (4.6) for Z_0 highlight the influence of the size of the network on its dynamics, through the number n of its nodes, and the impact of the topology, through the factor

$$\sup_{\mathscr{R}} |\mathcal{L}|,$$

where $\mathcal{L}$ is the coupling operator defined by (2.21). Thus, it is reasonable to expect that a large network would exhibit various complex dynamics. Furthermore, it is seen that the constant k_0 can approach 0 if only one node i in the network admits a low value for one of its parameters $B^{(i)}$, $C_2^{(i)}$ or $C_1^{(i)}$. Such a node could drive the rest of the network to an inappropriate dynamics, with a propagation of panic for instance.

Now we are ready to prove the existence of attractors for both problems (2.12) and (2.18). If $\big(S(t), Z, X\big)$ denotes a continuous dynamical system defined in a Banach space X, with phase space $Z \subset X$, we recall that a subset $\mathfrak{a} \subset Z$ is a 'global attractor' of $\big(S(t), Z, X\big)$ if $\mathfrak{a}$ is compact, invariant and attracts bounded subsets of Z (Yagi, 2009; Temam, 2012). May it exist, such an attractor is necessarily unique. Furthermore, a subset $\mathfrak{m} \subset Z$ is said to be an 'exponential attractor' of $\big(S(t), Z, X\big)$ if it is a positively invariant, compact subset of Z containing the global attractor, which attracts bounded subsets of Z at an exponential rate.

THEOREM 5 Under the assumptions of Theorem 3 and Proposition 3, the semi-group of nonlinear operators $S(t)$ defined by (3.12) determines a continuous dynamical system $(S(t), \tilde{Z}, X)$ with a compact phase space $\tilde{Z} \subset Z$, which admits a global attractor $\mathfrak{a}$, and a family $\mathfrak{m}$ of exponential attractors that contain $\mathfrak{a}$.

Proof. The estimates (4.2) guarantee that the semi-group $S(t)$ is continuous in $L^2(\Omega, R_{\alpha,\beta})$. Furthermore, since X is a Hilbert space, and $\mathcal{D}(A)$ is compactly embedded in X, it is proved in Yagi (2009, Chapter 6, Section 5.4) that the so-called 'squeezing property' follows from the energy estimates (4.2). Then by Theorem 6.15 in Yagi (2009), we can conclude that there exists a compact subset $\tilde{Z}$ of Z such that $(S(t), \tilde{Z}, X)$ admits a family $\mathfrak{m}$ of exponential attractors that contain $\mathfrak{a}$. □

We have a similar result for the network problem (2.18).

THEOREM 6 Under the assumptions of Theorem 4 and Proposition 4, the semi-group of nonlinear operators $\mathscr{S}(t)$ defined by (3.13) determines a continuous dynamical system $\big(\mathscr{S}(t), \widetilde{\mathscr{Z}}, X\big)$ with a compact phase space $\widetilde{\mathscr{Z}}$, which admits a global attractor $\mathfrak{A}$ and a family $\mathfrak{M}$ of exponential attractors that contain $\mathfrak{A}$.

It is worth noting that the latter attractors $\mathfrak{a}$, $\mathfrak{m}$, $\mathfrak{A}$ and $\mathfrak{M}$, which describe all the possible asymptotic behaviours of the corresponding semi-groups, have a finite fractal dimension (see Efendiev *et al.*, 2004; Temam, 2012; Miranville & Quintanilla, 2015), which can be evaluated in terms of the parameters involved in the corresponding systems. The exponential attractors of both families $\mathfrak{m}$ and $\mathfrak{M}$ are larger than the global attractors $\mathfrak{a}$ and $\mathfrak{A}$, respectively, but they are more robust to a variation of the parameters contained in the systems. Furthermore, it is known (see Eden *et al.*, 1994) that this fractal dimension can be estimated by a proportional to $|\Omega|$ quantity, for some particular reaction–diffusion equations. Thus, it seems reasonable to expect that the fractal dimension of the exponential attractors, in the case of the network problem, should be estimated by a quantity that would be proportional to the number n of nodes in the subsequent graph. This work in progress will be presented in a separate paper.

5. Numerical simulations

In this section, we illustrate our theoretical results by numerical simulations of both problems (2.12) and (2.18) using a splitting scheme (see Strang, 1964 or Descombes, 2001). As mentioned above, those simulations have been prepared with the collaboration of geographers (Provitolo *et al.*, 2015; Cantin *et al.*, 2017) and are related to the realistic scenario of a tsunami on the Mediterranean coast.

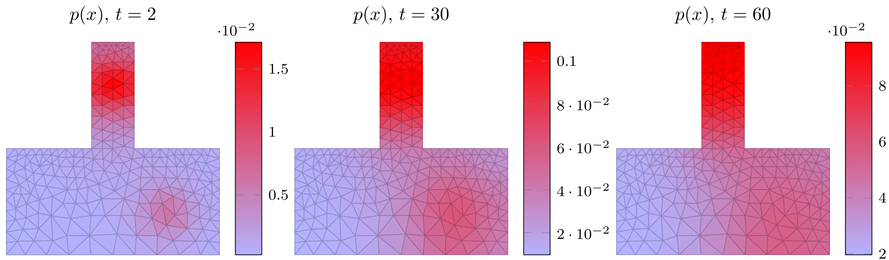

FIG. 2. Numerical simulation of problem (2.12) on a domain Ω that models a beach of the Mediterranean coast evacuated by a corridor (first case). At $t = 0$, individuals in daily behaviour q are located on the beach or within the corridor, and individuals in control behaviour c are located within the corridor. The presence of individuals in control behaviour c within the corridor tempers the spreading of panic p on the beach.

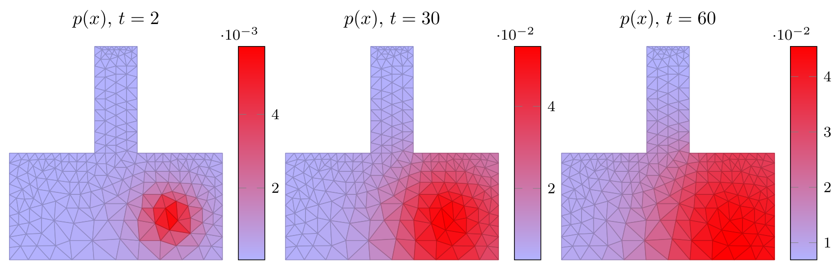

FIG. 3. Numerical simulation of problem (2.12) on a domain Ω that models a beach of the Mediterranean coast evacuated by a corridor (second case). At $t = 0$, individuals in daily behaviour q are located only on the beach. We observe that panic spreads on the beach, and it seems that individuals are incapable of finding the exit of the area exposed to the risk.

5.1 *Simulation of panic on a beach evacuated by a corridor*

We begin with a numerical simulation of problem (2.12) on a domain Ω (depicted on Figs 2 and 3), which models a beach of the Mediterranean coast, evacuated by a corridor. This scenario is of great interest, since it is known that a submarine fracture, located at about 50 km from the littoral, can provoke submarine earthquakes which in turn generate tsunamis of middle intensity (see Ioualalen *et al.*, 2014). The landscape of the coast is characterized by small beaches, which are connected to urban installations by step corridors of variable sizes. For example, the beaches of Nice city (France) are connected to the famous avenue ‘Promenade des Anglais’ by dozens of step corridors. Furthermore, the urban areas that are located behind the beaches admit an elevation with respect to the sea level; this elevation seems to be sufficient to favour a feeling of security, which is likely to bring individuals to evolve from panic to control behaviour.

We fix $\gamma = \varphi = 1$, $B_1 = B_2 = 0.4$, $C_1 = C_2 = 0.2$; $f = g = 0$, $h = 0.5$, which means that we neglect imitation between control and reflex or between panic and reflex, and favour imitation from panic to control; $d_2 = 25$, $d_1 = d_3 = d_4 = 1$, which means that we suppose that displacements of individuals in control behaviour are faster than displacements of individuals in other behaviours. The domain Ω is obtained by juxtaposition of a rectangle of dimensions $L \times \frac{1}{2}L$ (with $L = 20.0$) modelling the beach, and a smaller rectangle of dimensions $\frac{1}{5}L \times \frac{1}{2}L$ modelling the corridor of evacuation. Furthermore, we distinguish two cases for the initial conditions.

First case. We assume for $t = 0$ that individuals in daily behaviour q are located on the beach or within the corridor, and individuals in control behaviour c are located within the corridor, thus we set

$$\begin{aligned} q_0(x, y) &= \left[1 + \left(x - \tfrac{3L}{4}\right)^2 + \left(y - \tfrac{L}{5}\right)^2\right]^{-1} + \left[1 + \left(x - \tfrac{L}{2}\right)^2 + \left(y - \tfrac{4L}{5}\right)^2\right]^{-1}, \\ c_0(x, y) &= \left[1 + \left(x - \tfrac{L}{2}\right)^2 + \left(y - \tfrac{4L}{5}\right)^2\right]^{-1}, \\ r_0 &= p_0 \equiv 0. \end{aligned}$$

The results of the numerical simulation, for the panic behaviour p at $t = 2$, $t = 30$, $t = 50$, are shown in Fig. 2. We observe that the presence of individuals in control behaviour within the corridor tempers the spreading of panic on the beach, which seems to be the consequence of the imitation phenomenon modelled by the quadratic term $+hcp$ in the second equation of system (2.1).

Second case. We assume for $t = 0$ that individuals in daily behaviour q are located only on the beach, thus we set

$$\begin{aligned} q_0(x, y) &= \left[1 + \left(x - \tfrac{3L}{4}\right)^2 + \left(y - \tfrac{L}{5}\right)^2\right]^{-1}, \\ r_0 &= c_0 = p_0 \equiv 0. \end{aligned}$$

The results of the numerical simulation, for the panic behaviour p at $t = 2$, $t = 30$, $t = 50$, are shown in Fig. 3. In this second case, it is clear that panic spreads on the beach, and it seems that individuals are incapable of finding the exit of the area exposed to the risk.

5.2 *Effect of the evolution parameter from panic to control*

We continue with a simulation of problem (2.12), on a circular domain Ω of radius $\rho = 10$. Here, our aim is to show that one can reproduce with the reaction–diffusion system (2.1) the dynamics of the original PCR, defined by a system of ordinary differential equations [see equation (1.1)], for which it has been proved that a persistence of panic occurs when the evolution parameter C_1 (from panic to control) is null. Thus, we fix

$$\begin{aligned} &\gamma = \varphi = 1, \quad B_1 = B_2 = 0.4, \quad C_1 = 0.02 \text{ or } 0.6, \\ &C_2 = 0.6, \quad d_1 = d_3 = d_4 = 1, \quad d_2 = 5, \quad \rho = 10, \end{aligned}$$

and we determine the initial conditions by setting

$$q_0(x, y) = \left[1 + (x - \rho)^2 + (y - \rho)^2\right]^{-1}, \quad r_0 = c_0 = p_0 \equiv 0,$$

which corresponds to the situation when all individuals are in the daily behaviour q before the catastrophe, with a population localized at the centre of the domain Ω. The values of B_1 and B_2 mean that the evolution processes from reflex to control, and from reflex to panic, respectively, are of similar intensity and are dominated by the evolution process from control to panic, modelled by C_2. As explained previously, the diffusion rate d_2 for the control behaviour is larger than the other diffusion rates.

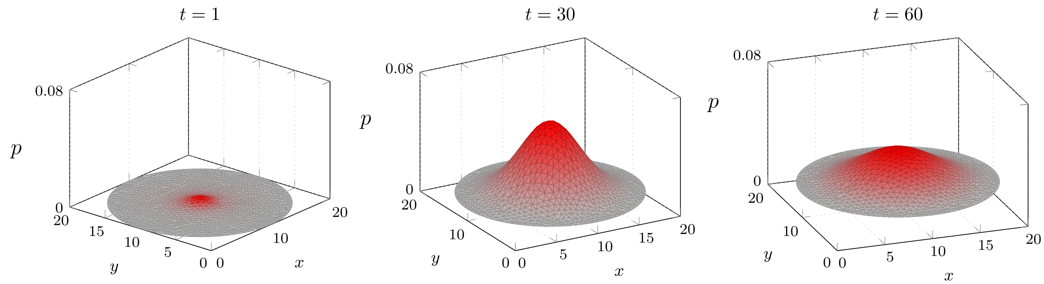

FIG. 4. Decrease of panic for a large value of the evolution parameter C_1 from panic to control after a transitional phase corresponding to the action of the catastrophe, during which the panic behaviour spreads in the affected population. The energy estimates given in Proposition (3) guarantee that the panic component exponentially decreases.

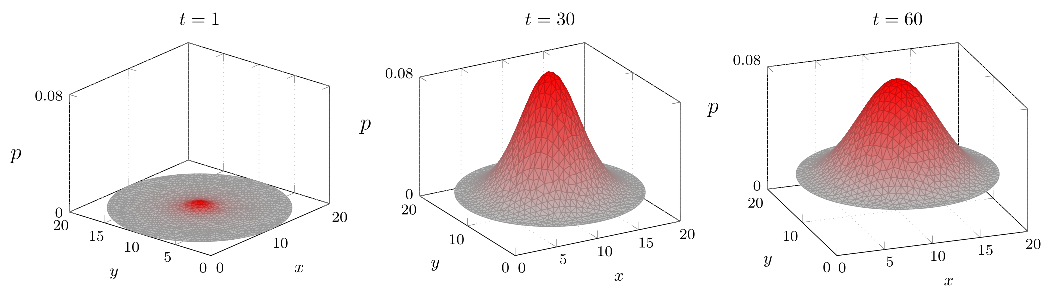

FIG. 5. Persistence of panic for a low value of the evolution parameter C_1 from panic to control. After the transitional phase, the panic level does not converge to 0, in particular in the neighbourhood of the boundary of Ω.

The results for the panic component p are depicted in Fig. 4 in the case $C_1 = 0.6$, and in Fig. 5 in the case $C_1 = 0.02$. As mentioned above, it is proved in Cantin *et al.* (2016) that a low value of the parameter C_1 is expected to provoke a high level of panic in the Ordinary Differential Equation (ODE) model. This pattern is recovered in the reaction–diffusion model (2.1), as illustrated in Fig. 5, where the level of the density of individuals in panic behaviour exhibits high values, whereas Fig. 4 shows that the panic level decreases for a higher value of C_1, after a transitional phase corresponding to the action of the catastrophe, during which the panic behaviour spreads in the affected population.

According to Proposition 3, we can compute the coefficients δ_1 and δ_2 involved in the energy estimates (4.1). In the case $C_1 = 0.02$, we have $\delta_1 = 0.78 > 0$, $\delta_2 = -0.96 < 0$, which is coherent with the fact that the panic behaviour does not decrease to 0. In particular, it is observed that the panic level increases in the neighbourhood of the boundary of Ω. However, the existence of an invariant region is guaranteed by Theorem 3, thus forbids an explosion in finite time for the panic behaviour. In the case $C_1 = 0.6$, we have $\delta_1 = \delta_2 = 0.2 > 0$, which accounts for the decrease of the panic behaviour observed in Fig. 4. This numerical experimentation shows that the spatial-temporal model given by the reaction–diffusion system (2.1) is able to reproduce basic patterns concretely discussed by geographers.

5.3 *Effect of the coupling orientation in a four nodes network*

We continue with numerical simulations of problem (2.18) in the case of a network composed with 4 nodes and experiment the effect of an inversion of the coupling orientation. We consider two nodes

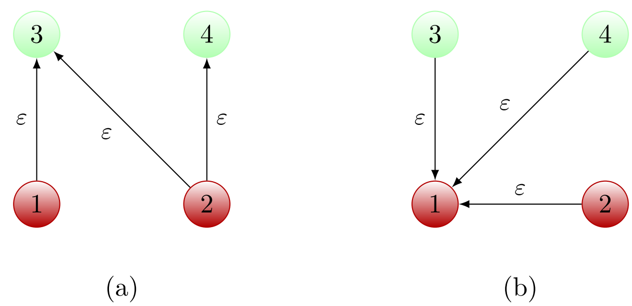

FIG. 6. PCR network composed with four nodes. (a) Evacuation of individuals of the nodes that are likely to exhibit a high level of panic in absence of coupling (nodes 1 and 2, coloured in dark red) towards the nodes that are known to have the capacity of absorbing the panic behaviour (nodes 3 and 4, coloured in light green). (b) Other configuration of the four nodes network, with a displacement of individuals towards a node that admits a high level of panic in absence of coupling.

(coloured in red in Fig. 6) for which the evolution parameter from panic to control C_1 admits a low value, coupled with two additional nodes for which C_1 is larger (coloured in green in Fig. 6). The initial conditions for each node are given by

$$q_0(x, y) = \left[1 + (x - \rho)^6 + (y - \rho)^6\right]^{-1}, \quad r_0 = c_0 = p_0 \equiv 0,$$

which corresponds to a pick of individuals in daily behaviour at the centre of the domain before the action of the catastrophe. The values of the parameters are

$$\gamma = \varphi = 1, \quad B_1 = 0.15, \quad B_2 = 0.9, \quad C_1 = 0 \text{ or } 0.3,$$
$$C_2 = 0.2, \quad d_1 = d_2 = d_3 = d_4 = 1, \quad \varepsilon = 1, \quad \rho = 10.$$

The first situation, depicted in Fig. 6a, corresponds to an evacuation of individuals of the nodes that are likely to exhibit a high level of panic in absence of coupling, towards the nodes that are known to have the capacity of absorbing the panic behaviour. The numerical results for the panic components p_1 and p_2 of the nodes 1 and 2, respectively, are shown in Fig. 7. It is observed that the panic level decreases on the two nodes 1 and 2, and the rate of decrease is faster on the node 2, due to the double evacuation of that node.

The second situation, presented in Fig. 6b, corresponds to another configuration of the coupling orientation. More precisely, we experiment a displacement of individuals of the nodes 2, 3 and 4 towards the node 1, which is likely to admit a high level of panic. The numerical results, given in Fig. 8, show that the panic behaviour is exacerbated on that node, whereas the panic behaviour on the node 2 is inhibited.

5.4 *Effect of a high ratio in diffusion rates with nonlinear imitation*

Finally, we experiment the possible emergence of spatial instabilities in the case of a high ratio in the diffusion rates. Thus, we consider a simple network of two nodes, with an imitation on the node 2 from

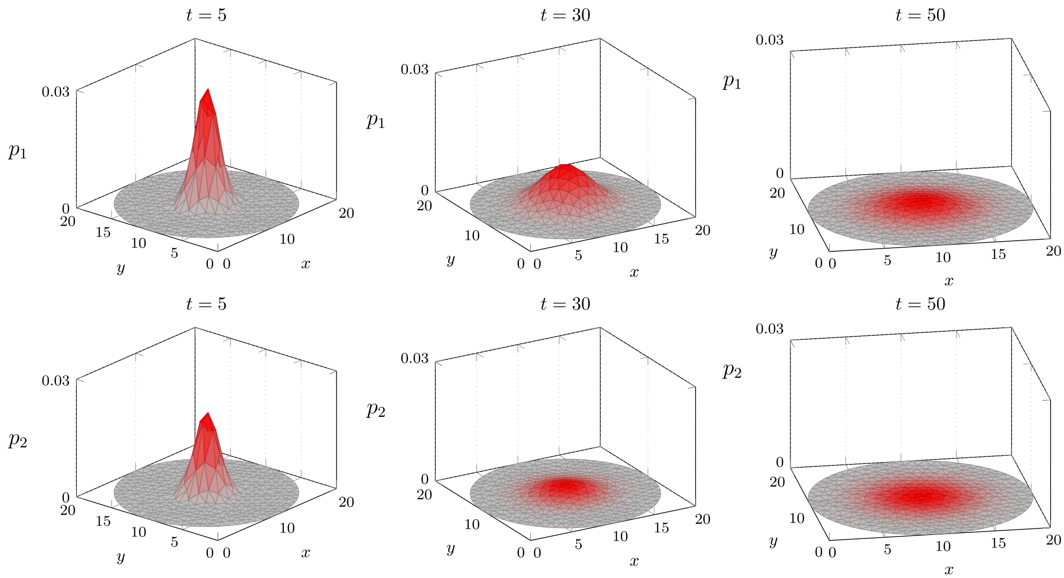

FIG. 7. Numerical results for the situation depicted in Fig. 6a. The first line shows the evolution of the panic density p_1 on the first line, and p_2 is depicted on the second line. The panic level decreases on the two nodes 1 and 2, and the rate of decrease is faster on the node 2, due to the double evacuation of that node.

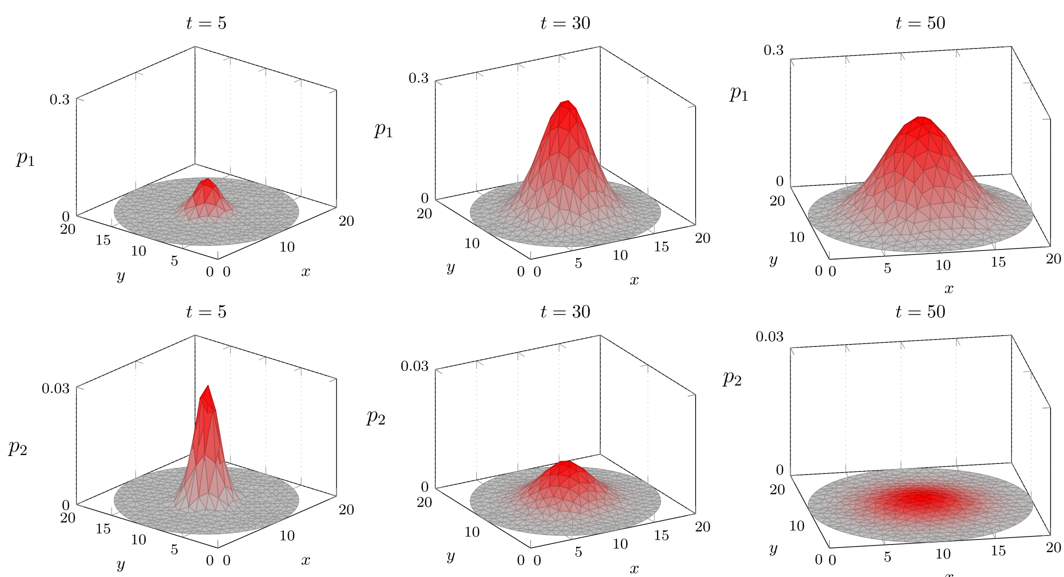

FIG. 8. Numerical results for the situation depicted in Fig. 6b. The panic behaviour p_1 on the node 1 (first line) is exacerbated, whereas the panic behaviour p_2 on the node 2 (second line) is inhibited.

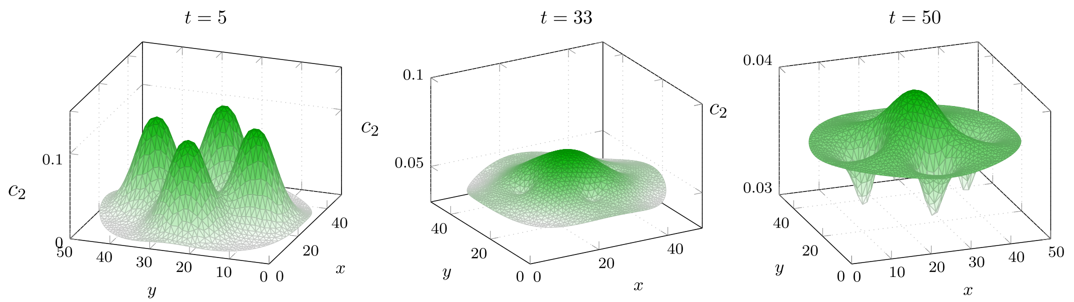

FIG. 9. Numerical simulation of a two-nodes networks with nonlinear imitation and a high ratio in the diffusion rates. Complex dynamics occur.

control towards panic, modelled by the nonlinear term $h\,c_2\,p_2$. The values of the parameters are

$$\gamma = 1, \quad \varphi = 0.01, \quad B_1 = 0.15, \quad B_2 = 0.9, \quad C_1 = 0.01, \quad C_2 = 0.2,$$
$$\varepsilon = h = 0.95, \quad d_1 = 15, \quad d_2 = 25, \quad d_3 = 0.1, \quad d_4 = 5, \quad \rho = 25.$$

We choose the diffusion rates by favouring the displacement of individuals in control behaviour, which corresponds to a rough approximation of the geographical observations. The initial conditions are given on each node by

$$\begin{aligned} q_0(x, y) = {} & \left[1 + \tfrac{1}{10}(x-\rho)^6 + \tfrac{1}{10}(y - \tfrac{1}{2}\rho)^6\right]^{-1} + \left[1 + \tfrac{1}{10}(x-\rho)^6 + \tfrac{1}{10}(y - \tfrac{3}{2}\rho)^6\right]^{-1} \\ & + \left[1 + \tfrac{1}{10}(x - \tfrac{3}{2}\rho)^6 + \tfrac{1}{10}(y-\rho)^6\right]^{-1} + \left[1 + \tfrac{1}{10}(x - \tfrac{1}{2}\rho)^6 + \tfrac{1}{10}(y-\rho)^6\right]^{-1}, \end{aligned}$$

and $r_0 = c_0 = p_0 \equiv 0$, which represents four picks of individuals in daily behaviour at the centre of the domain, before the action of the catastrophe.

The numerical results for the control component c_2 of the node 2 are presented in Fig. 9. We observe that the areas where the control behaviour admits a high level at the beginning of the evolution process are subject to the nonlinear imitation process from control to panic, thus a reversal of the proportions in the panic and control behaviours. Meanwhile, the entering coupling with the node 1 guarantees an intake of individuals on the node 2, the weak value of φ inhibits the behavioural purge, and the high diffusion rate d_2 for the control behaviour provokes the diffusion of individuals in control behaviour in the whole domain Ω, at a speed that is greater than the diffusion of individuals in panic behaviour. Thus, the level of control behaviour becomes predominant at the centre of the domain, where the nonlinear imitation process from control to panic cannot occur, since the individuals in panic do not reach this area sufficiently fast. Roughly speaking, the superposition of reaction, diffusion, coupling and nonlinear imitation lets complex dynamics occur. It is a work in progress to exhibit other complex dynamics, such as damped oscillations, in coupled networks of higher size.

6. Conclusion and perspectives

In this work, we have presented the mathematical analysis of an evolution problem given by a coupled network of reaction–diffusion systems, modelling human behaviours during catastrophic events. Existence, uniqueness, non-negativity and boundedness, which are obvious properties to be satisfied, are now rigorously proved. Numerical simulations concord with the geographical background of our model. The study of the asymptotic dynamics is related to the existence of exponential attractors, which follows from energy estimates. In a forthcoming paper, we shall present the continuation of our research, with an estimation of the fractal dimension of those attractors, which seems to be linked to the size of the network, an exploration of the possible bifurcations occurring in the system and an improvement of our modelling obtained by coupling reaction–diffusion systems defined on non-identical domains.

Acknowledgements

The authors are very grateful to the anonymous reviewers whose comments greatly improved the presentation of the paper.

Funding

Région Normandie and the UCA-JEDI Investments in the Future project managed by the National Research Agency (ANR) (ANR-15-IDEX-01).

References

Adams, R. A. & Fournier, J. J. F. (2003) *Sobolev Spaces*, vol. **140**. Oxford: Academic Press.

Ambrosio, B., Aziz-Alaoui, M. A. & Phan, V. L. E. (2019) Large time behaviour and synchronization of complex networks of reaction–diffusion systems of Fitzhugh–Nagumo type. *IMA J. Appl. Math.*, **84**, 416–443.

Cantin, G. (2017) Nonidentical coupled networks with a geographical model for human behaviors during catastrophic events. *Internat. J. Bifur. Chaos*, **27**, 1750213.

Cantin, G., Verdière, N., Lanza, V., Aziz-Alaoui, M. A., Charrier, R., Bertelle, C., Provitolo, D. & Dubos-Paillard, E. (2016) Mathematical modeling of human behaviors during catastrophic events: stability and bifurcations. *Internat. J. Bifur. Chaos*, **26**, 1630025.

Cantin, G., Verdière, N., Lanza, V., Aziz-Alaoui, M. A., Charrier, R., Bertelle, C., Provitolo, D. & Dubos-Paillard, E. (2017) Control of panic behavior in a non identical network coupled with a geographical model. *PhysCon 2017*. Singapore: University Firenze, pp. 1–6.

Caraballo, T., Lukaszewicz, G. & Real, J. (2006) Pullback attractors for asymptotically compact non-autonomous dynamical systems. *Nonlinear Anal.*, **64**, 484–498.

Chen, G., Wang, X. & Li, X. (2014) *Fundamentals of Complex Networks: Models, Structures and Dynamics*. Singapore: John Wiley & Sons.

Descombes, S. (2001) Convergence of a splitting method of high order for reaction-diffusion systems. *Math. Comp.*, **70**, 1481–1501.

Eden, A., Foias, C., Nicolaenko, B. & Temam, R. (1994) *Exponential Attractors for Dissipative Evolution Equations*. Research in Applied Mathematics.

Efendiev, M., Miranville, A. & Zelik, S. (2004) Infinite-dimensional exponential attractors for nonlinear reaction–diffusion systems in unbounded domains and their approximation. *Proc. R. Soc. A*, **460**, 1107–1129.

Efendiev, M., Zelik, S. & Miranville, A. (2005) Exponential attractors and finite-dimensional reduction for non-autonomous dynamical systems. *Proc. Roy. Soc. Edinburgh Sect. A*, **135**, 703–730.

Haase, M. (2006) *The Functional Calculus for Sectorial Operators*. pp. 19–60.

Hale, J. K. (1997) Diffusive coupling, dissipation, and synchronization. *J. Dynam. Differential Equations*, **9**, 1–52.

Ioualalen, M., Larroque, C., Scotti, O. & Daubord, C. (2014) Tsunami mapping related to local earthquakes on the French-Italian Riviera (Western Mediterranean). *Pure Appl. Geophys.*, **171**, 1423–1443.

Li, X., Jiang, W. & Shi, J. (2013) Hopf bifurcation and Turing instability in the reaction–diffusion Holling–Tanner predator–prey model. *IMA J. Appl. Math.*, **78**, 287–306.

Miranville, A. and Quintanilla, R. (2015) A generalization of the Allen–Cahn equation. *IMA J. Appl. Math.*, **80**, 410–430.

Murray, J. D. (2002) *Mathematical Biology I: An Introduction*. Interdisciplinary Applied Mathematics, vol. 17. New York, NY, USA: Springer.

Okubo, A. (1980) Diffusion and ecological problems: mathematical models. *BIOMATH*, **10**.

Pierre, M. (2010) Global existence in reaction–diffusion systems with control of mass: a survey. *Milan J. Math.*, **78**, 417–455.

Provitolo, D., Dubos-Paillard, E., Verdière, N., Lanza, V., Charrier, R., Bertelle, C. & Aziz-Alaoui, M. A. (2015) Les comportements humains en situation de catastrophe: de l'observation à la modélisation conceptuelle et mathématique. *Cybergeo*, **735**.

Rothe, F. (1984) Global solutions of reaction–diffusion systems. *Lecture Notes in Math.*, **1072**.

Ruan, S. (1998) Turing instability and travelling waves in diffusive plankton models with delayed nutrient recycling. *IMA J. Appl. Math.*, **61**, 15–32.

Sherratt, J. A. (2008) A comparison of periodic travelling wave generation by Robin and Dirichlet boundary conditions in oscillatory reaction–diffusion equations. *IMA J. Appl. Math.*, **73**, 759–781.

Smoller, J. (1994) *Shock Waves and Reaction–Diffusion Equations*, vol. **258**. New York: Springer Science & Business Media.

Strang, G. (1964) Accurate partial difference methods. *Numer. Math.*, **6**, 37–46.

Temam, R. (2012) *Infinite-Dimensional Dynamical Systems in Mechanics and Physics*, vol. **68**. New York: Springer Science & Business Media.

Verdière, N., Cantin, G., Provitolo, D., Lanza, V., Dubos-Paillard, E., Charrier, R., Aziz-Alaoui, M. A. & Bertelle, C. (2015) Understanding and simulation of human behaviors in areas affected by disasters: from the observation to the conception of a mathematical model. *Global J. Hum. Soc. Sci.*, **15**, 7–15.

Wang, J. L., Wu, H. N., Huang, T. & Ren, S. Y. (2018) *Analysis and Control of Coupled Neural Networks with Reaction–Diffusion Terms*. Singapore: Springer.

Yagi, A. (2009) *Abstract Parabolic Evolution Equations and Their Applications*. Berlin Heidelberg: Springer Science & Business Media.

Yang, X., Cao, J. & Yang, Z. (2013) Synchronization of coupled reaction–diffusion neural networks with time-varying delays via pinning-impulsive controller. *SIAM J. Control Optim.*, **51**, 3486–3510.